Electric Power Systems Research 212 (2022) 108475

Contents lists available at ScienceDirect

Electric Power Systems Research

journal homepage: www.elsevier.com/locate/epsr

Local voltage control in distribution networks using PI control of active and reactive power☆

Martin Lundberg [a,*], Olof Samuelsson [a], Emil Hillberg [b]

[a] Industrial Electrical Engineering and Automation, Lund University, Lund, Sweden
[b] Electric Power Systems, RISE Research Institutes of Sweden, Göteborg, Sweden

ARTICLE INFO

Keywords:
Distribution networks
Control algorithms
Local voltage control
Stability analysis

ABSTRACT

Overvoltage is becoming increasingly prevalent in distribution networks with high penetration of renewable distributed energy sources (DERs). Local control of converter-based resources is a flexible and scalable method to prevent this growing issue. Reactive power is used for voltage control in many local control schemes. However, the typical range of R/X ratios for distribution power lines indicates that mitigation of overvoltage often requires excessive amounts of reactive power. Complete reliance on reactive power thus limits the effectiveness of local control strategies. In this work we instead propose a method that combines enhanced power factor voltage control with upper voltage limit tracking using PI control. We develop a modelling framework and demonstrate the stability of the proposed method. We then simulate the nonlinear operation of two parallel PI controllers in a medium voltage test system.

1. Introduction

In power distribution networks (DNs) with large shares of nondispatchable distributed energy resources (DERs), such as solar and wind power plants, elevated voltage levels can be observed at times when large generation coincides with low demand. This poses a challenge for distribution system operators (DSOs) who must ensure sufficient power quality during operation. The control capabilities of converter-based DERs can be used to eliminate voltage constraint violations, and extensive physical network upgrades can thereby be mitigated or deferred.

1.1. Voltage control in distribution networks

Many DSOs rely on network reinforcement and subsequent on-load tap changer corrections [1] to keep voltages within prescribed limits (typically ±5% or ±10% deviation from nominal voltage, e.g.[2]). Consequently, voltage management then becomes a mainly offline design issue based on worst-case operating conditions and reliance on significant operational margins — a strategy sometimes referred to as *fit-and-forget*. The large-scale introduction of converter-based DERs has made it possible to transition to active network management and online control with the potential to safely reduce margins to increase overall grid utilization [3]. This change in perception is exemplified by the inclusion of DER control schemes in various grid codes and standards [4–6].

A wide range of voltage control algorithms for DERs has been presented in literature. Droop-like schemes based on local measurements, including the use of volt/var or volt/watt curves, have been extensively researched [7–9], and similar schemes have been included in the aforementioned grid codes. Various voltage control optimization methods involving droop curve parameters [10], centralized control [11], and distributed control [12] have also been suggested. The key factor for performance enhancement in all cases is the ability to distribute individual DER controller set points. Online coordination typically demands communications infrastructure together with modern cybersecurity protocols that are not present in many DNs today. The resulting increase in implementation complexity – and its associated costs – must be factored in when considering actual deployment of improved voltage control methods, particularly in the presence of a large number of small-scale distributed generators, such as roof-top photovoltaic units.

Therefore, solutions that are sub-optimal from a strictly operational perspective can still be preferred by DSOs if they are simple, scalable, and aligned with existing network regulations. The absence of extensive communications infrastructure in local control schemes also makes them suitable for *plug-and-play* implementations, which permit the

☆ This work has been carried out within the framework of the ANM4L project Hillberg et al. (2020), which is supported by EU H2020 grant agreement No 775970 through the ERA-Net SES initiative.

* Corresponding author.
E-mail addresses: martin.lundberg@iea.lth.se (M. Lundberg), emil.hillberg@ri.se (E. Hillberg).

https://doi.org/10.1016/j.epsr.2022.108475
Received 3 October 2021; Received in revised form 16 April 2022; Accepted 2 July 2022
Available online 20 July 2022
0378-7796/© 2022 The Authors. Published by Elsevier B.V. This is an open access article under the CC BY license (http://creativecommons.org/licenses/by/4.0/).

introduction and removal of units with minimal need for reconfiguration of other network controllers [13], an attractive option in rapidly evolving DNs with increased planning uncertainties.

1.2. Decentralized control

We categorize three types of local voltage control strategies described in the literature after their respective objectives.

Supporting strategies aim at reducing the voltage increase during normal operation through actions taken primarily within the allowed voltage range. Most volt/var and volt/watt droop curves, both static [8] and incremental [14], belong to this category. Such controllers act before any voltage limits have been exceeded, making curtailment less favourable due to the reduced utilization of DERs. However, the effectiveness of reactive power strategies, such as volt/var, are restricted by power factor limitations set by off-the-shelf DER converters [15], creating a need for oversized equipment. Furthermore, network loading limits put additional restrictions on reactive power usage on a system level.

Set point tracking strategies, e.g.[16], follow predetermined voltage reference signals. Decentralized set point tracking is complicated by the inevitable interactions between individual controllers caused by the physical connection of grid components. As pointed out in [10], decoupling of controllers to achieve the desired performance is not always feasible.

Limitation strategies, much like support schemes, do not track a certain voltage set point and instead act as disturbance rejection controllers. The difference being that with a limitation strategy control actions are restricted to when voltage constraint violations occur. This category includes the type of incremental volt/var curve presented in [17], as was observed in [12]. Limitation strategies typically involve a smaller number of units since only DERs experiencing overvoltage contribute to the control effort [12]. Thus, the effectiveness is limited by the underutilization of available resources.

1.3. Active and reactive power injections

While both active (P) and reactive (Q) power injections from DERs impact the network voltage level, controlling Q is often preferred in the mentioned voltage control strategies as curtailment is associated with revenue losses for producers. The maximum amount of reactive power is then typically needed when the active power injections reach their peak, which might be an unattainable requirement due to the earlier mentioned converter and/or network limits. Failing to mitigate overvoltage can result in inverter tripping, as has been observed in actual operation [18], leading to uncontrolled curtailment of the affected DER units.

The relative effectiveness of using P or Q for voltage control depends on the relation between the resistance and reactance of the network power lines, also known as the R/X-ratio. In European distribution networks typical R/X-ranges are 0.40–2.00 (MV) and 0.70–11.00 (LV) [19], which implies that active power can be as much as 11 times as effective in controlling the voltage magnitude as reactive power. Thus, the total control effort could potentially be reduced considerably by including curtailment in the control scheme.

Given the potential negative financial impact of curtailment, a monetary compensation scheme linked to actual control efforts should be considered. Accurate tracking of the maximum potential DER active power injections would allow for individual metering. Real-time estimation techniques developed for wind power plants, e.g.[20], and photovoltaic systems [21] make it possible not only to track the maximum potential instantaneous generation but also to use it as a reference for a local controller. This approach is referred to as delta control in [21,22].

1.4. Contributions

In this paper we propose and evaluate a decentralized voltage control method combining three strategies: *support* with reactive power, single-sided *set point tracking* of the upper voltage limit, and *limitation* using delta control. The method allows for increased control performance while use of curtailment is limited to when reactive power control is insufficient to prevent voltage constraint violations.

2. Dynamic models

In this section we present a local control scheme and establish a general modelling framework for evaluation of the proposed method.

2.1. Distribution network model

Following [14] we consider a balanced and symmetric radial DN with n buses. Each bus $i \in N$ with $N = \{1, \dots, n\}$ is characterized by the 4-tuple $(v_i, \theta_i, p_i, q_i)$ where v_i is the line-to-line rms voltage; θ_i the voltage phase angle relative θ_1; p_i and q_i the P and Q injections. Bus 1 is connected to an overlying network and is modelled as a slack bus with constant voltage magnitude and angle. The remaining buses are defined as pq-buses with known active and reactive power output. We approximate the influence of power injections on network voltages by linearization of the power flow Eqs. (1) around a steady state operating point $(v^0, \theta^0, p^0, q^0)$, where v, θ, p and q are vectors consisting of all of their respective bus elements such that

$$\begin{bmatrix} \Delta p \\ \Delta q \end{bmatrix} \approx \mathcal{J}(v, \theta) \begin{bmatrix} \Delta v \\ \Delta \theta \end{bmatrix}, \tag{1}$$

where $\mathcal{J} \in \mathbf{R}^{2n \times 2n}$ is the network Jacobian. For small deviations from the operating we let $p = p^0 + \Delta p$ (and similarly for v, θ and q). We can then rewrite (1) as

$$\begin{bmatrix} \Delta v \\ \Delta \theta \end{bmatrix} = \mathcal{J}(v, \theta)^{-1} \begin{bmatrix} \Delta p \\ \Delta q \end{bmatrix}, \tag{2}$$

which requires the Jacobian to be invertible — a reasonable assumption if the operating point has been determined by solving the power flow equations with the Newton–Raphson method. From here on we only consider the parts of (2) affecting the voltage magnitude. For simplicity the pq-buses are classified as *either* generation buses or load buses, yielding the vector decomposition $v = [v^{slack}, v^{gen}, v^{load}]^T$, $p = [p^{slack}, p^{gen}, p^{load}]^T$ and $q = [v^{slack}, q^{gen}, q^{load}]^T$. Locally controlled DERs are added to all generation nodes and the controllers are synchronized so that all input–output updates occur at universal time-discrete instances. At each time step t_k each controller measures the local voltage and updates the DER P and Q set points. The set points are kept constant until the next time instance t_{k+1}. It is assumed that all adjustments within a converter operating range are both fast and stable and that the dynamics of all converters, loads, and network components, stemming from variations at t_k, have settled before the next time step, yielding steady state voltages at t_{k+1}. This approach is aligned with [14] and is motivated by the discrete-time nature of digital controllers combined with the time-scale separation of the local DER control loop from other types of fast network dynamics, with the former having a significantly larger time constant.

2.2. DER model and delta control

The converter active power set point of a DER at bus i is determined as

$$p_i^{gen} = \tilde{p}_i^{gen} + \delta p_i^{gen}, \tag{3}$$

with $\tilde{p}_i^{gen}$ being the estimated DER maximum power injection and δp_i^{gen} the delta control signal, where $\delta p_i^{gen} \leq 0$. The reactive power set point, q_i^{gen}, is adjusted for voltage control. We select it based on the potential

active power injection $\tilde{p}_i^{gen}$ and a predefined constant power factor, $cos(\varphi)$, such that

$$q_i^{gen} = -tan(arccos(cos(\varphi)))\tilde{p}_i^{gen} = C_i^{pf}\tilde{p}_i^{gen}. \quad (4)$$

For a network with m controlled DERs, with $m \in M = \{2, \dots, m\} \subset N$, we can use (2), and (4) to define the matrices $K^c, \tilde{K}^c \in \mathbf{R}^{n\times m}$ with each element containing the sensitivity of a voltage v_h, $h \in N$, to an active power injection p_k^{gen}, $k \in M$, so that

$$K_{h,k}^c = \frac{\partial v_h}{\partial p_k}, \quad (5)$$

$$\tilde{K}_{h,k}^c = \frac{\partial v_h}{\partial p_k} + C_i^{pf}\frac{\partial v_h}{\partial q_k}. \quad (6)$$

Using (3), (5) and (6) the potential influence of the maximum DER power injections on bus voltages can be separated from the impact of delta control actions as

$$\tilde{K}^c\tilde{p}^{gen} + K^c\delta p^{gen}, \quad (7)$$

where $\tilde{p}^{gen}, \delta p^{gen} \in \mathbf{R}^m$. An open-loop model of the entire system is made by using (2), (7) and defining a vector $\tilde{v} \in \mathbf{R}^n$, where each element $\tilde{v}_h$ describes the maximum potential influence of noncontrollable power injections at t_k on the steady state voltage v_h at t_{k+1} given linearization around an operating point, i.e. $\tilde{v}_h = f_h(t_k, v^0, p^0, q^0, p^{load}, q^{load}, C_i^{pf}, \tilde{K}^c, \tilde{p}^{gen})$. A quasi-dynamic model (8) then be obtained:

$$v(t_{k+1}) = K^c\delta p^{gen}(t_k) + \tilde{v}(t_k). \quad (8)$$

(K^c can now be viewed as the open loop gain from δp^{gen} to v, and $\tilde{v}$ as process noise.)

2.3. Decentralized PI controller

We start with a general linear discrete-time single-input-single-output (SISO) PI controller of the form (9) that uses zero-order hold (ZOH) integration of the input signal e and generates the output signal u. An equivalent difference equation can be written as shown in (10) such that

$$u(t_k) = K\left(e(t_k) + \frac{T}{T_I}\sum_{i=0}^{k} e(t_i)\right), \quad (9)$$

$$u(t_k) = u(t_{k-1}) + K\left(e(t_k) - e(t_{k-1}) + \frac{T}{T_I}e(t_k)\right). \quad (10)$$

Here T is the sampling interval and $\{K, T_I\}$ design parameters. We extend the model to include multiple parallel SISO PI controllers by defining, for $k \in M$, $u_k := \delta p_k^{gen}$ and $e_k := v_k^r - v_k$. Since we want to curtail power in case of overvoltage, we let $v_k^r = v_{grid,k}^{max}\ \forall k$, where each element of the constant vector v_{grid}^{max} contains the network upper voltage limit. Furthermore, we assume that all controllers can be tuned identically in accordance with the *plug-and-play* strategy. Then we can write the matrix difference equation for the parallel PI controllers as

$$\delta p^{gen}(t_k) = \delta p^{gen}(t_{k-1}) + \alpha v^{gen}(t_k) + \beta v^{gen}(t_{k-1}) + \gamma, \quad (11)$$

with the scalar coefficients $\alpha = -\left(K + \frac{T}{T_I}\right)$, $\beta = K$ and the vector $\gamma = K\frac{T}{T_I}v_{grid}^{max}$.

There are physical limits that affect the range of the linear controller model (11). A PI controller acting on voltage signals below the upper limit tries to increase the DER output, which is unfeasible unless some power previously has been curtailed. At the other end, curtailment cannot exceed the actual real-time output. This can be thought of as a saturation of the converter active power injection such that $0 \le p_k^{gen} \le \tilde{p}_k^{gen}$ or equivalently $-\tilde{p}_k^{gen} \le \delta p_k^{gen} \le 0$. The upper delta control limit is particularly detrimental to the linear PI controller performance as it causes integrator wind-up during operation within the acceptable voltage range. A straight-forward approach to avoid this problem is to implement an anti-windup scheme directly related to the converter saturation limits so that

$$u(t_k) = [\delta p_k^{gen}(t_k)]_{-\tilde{p}_k^{gen}(t_k)}^{0}, \quad (12)$$

since feedforward of the potential DER maximum power injection is possible.

2.4. Closed-loop system

The system (8) can be reformulated as a state space model on the form (13), (14), where $x(t_k) = v(t_k)$ and $u(t_k) = \delta p^{gen}$. The decentralized PI controllers (11) can be realized as a state feedback controller of the form $u(t_k) = Lx(t_k) + \tilde{r}$ with $x(t_k) = [v^{gen}(t_k), \delta p^{gen}(t_{k-1}), v^{gen}(t_{k-1})]^T$ by augmenting the system dynamics to include the controller states. We now have

$$x(t_{k+1}) = Ax(t_k) + Bu(t_k) + N\tilde{v}(t_k); \quad (13)$$

$$y(t_k) = Cx(t_k), \quad (14)$$

where we are only considering nodes with DERs present, i.e. $A \in \mathbf{R}^{3m\times 3m}$, $B, N \in \mathbf{R}^{3m\times m}$, $C \in \mathbf{R}^{m\times 3m}$. Under influence of input saturation the system is piece-wise linear and (13) is updated as

$$x(t_{k+1}) = Ax(t_k) + B(t_k)u(t_k) + N\tilde{v}(t_k) + d(t_k), \quad (15)$$

where in case of saturation, that is, if any $u_k > 0$ or $u_k < -\tilde{p}_k^{gen}$, (13) becomes (15). The input matrix $B(t_k)$ is then updated so that the saturated input is negated by replacing it with a zero element. If $u_k < -\tilde{p}_k^{gen}$, then the vector $d(t_k)$ is introduced so that $d_j = -\tilde{p}_k^{gen}\ \forall j : m < j \le 2m$, where $d \in \mathbf{R}^{3m}$. If we expect that the number of saturated states to remain constant for the time $t_k \rightarrow t_{k+n}$ we can replace (15) with the more compact

$$\hat{x}(t_{k+1}) = \hat{A}(t_k)\hat{x}(t_k) + \hat{B}(t_k)\hat{u}(t_k) + \hat{N}(t_k)\hat{\tilde{v}}(t_k) + \hat{d}(t_k), \quad (16)$$

where $dim(\hat{\cdot}) \le dim(\cdot)$. Then (16) becomes the closed loop system for all unsaturated controllers with an added constant for the impact of the saturated controllers. In case of saturation, (16) is determined from (13) by removal of every k:th row and, if applicable, every k:th column of each entity of (13). Note that (15) and (16) are valid as a representation of the dynamics in (13) as long as the number of saturated states does not change. This will be discussed in more detail in the next section. First, we conclude the modelling section by giving an expression for the closed loop system, using (16) so that

$$\begin{aligned}\hat{x}(t_{k+1}) &= (\hat{A}(t_k) + \hat{B}(t_k)\hat{L}(t_k))\hat{x}(t_k)\\ &+ \hat{B}(t_k)\hat{r}(t_k) + \hat{N}(t_k)\hat{\tilde{v}}(t_k) + \hat{d}(t_k).\end{aligned} \quad (17)$$

Through the system matrix $\hat{A} + \hat{B}\hat{L}$ the impact of control loop interactions on the stability of solutions to (17) in a subspace of state space can be evaluated.

3. Stability

We observe that every system (17) has a feasible equilibrium. If the P and Q drawn by the loads as well as $\tilde{p}^{gen}(t_k)$ are constant, the equilibrium $(\delta\hat{p}^{gen,*}, \hat{v}^{gen,*})$ for a set of local PI controllers (11) acting on the system (13) with a constant number of unsaturated states in (16) is determined from (17). Equivalently, we can use the closed loop system obtained by combining the bus voltage measurements, given by (8), and the PI controllers on the form (11) so that

$$\begin{aligned}\delta\hat{p}^{gen}(t_{k+1}) &= \delta\hat{p}^{gen}(t_k) + \alpha[\hat{K}^c\delta\hat{p}^{gen}(t_k) + \hat{\tilde{v}} + \hat{d}]\\ &+ \beta[\hat{K}^c\delta\hat{p}^{gen}(t_{k-1}) + \hat{\tilde{v}} + \hat{d}] + \hat{\gamma}.\end{aligned} \quad (18)$$

The equilibrium curtailment is then found from

$$\begin{aligned}\delta\hat{p}^{gen,*} &= \delta\hat{p}^{gen,*} + \alpha[\hat{K}^c\delta\hat{p}^{gen,*} + \hat{\tilde{v}} + \hat{d}]\\ &+ \beta[\hat{K}^c\delta\hat{p}^{gen,*} + \hat{\tilde{v}} + \hat{d}] + \hat{\gamma},\end{aligned} \quad (19)$$

which, after some manipulation, yields

$$\delta\hat{p}^{gen,*} = (\hat{K}^c)^{-1}(\hat{v}^{max}_{grid} - \hat{v} - \hat{d}), \tag{20}$$

where $\hat{K}^c$ is assumed to be invertible. Consequently, the equilibrium voltage is

$$\begin{aligned} &\hat{v}^{gen,*} = \hat{K}^c(\hat{K}^c)^{-1}(\hat{v}^{max}_{grid} - \hat{v} - \hat{d}) + \hat{v} + \hat{d} \\ &\rightarrow \hat{v}^{gen,*} = \hat{v}^{max}_{grid}, \end{aligned} \tag{21}$$

which is the vector of reference signals for the controllers. The equilibrium voltages of the remaining network buses can then be determined by plugging (20) into (8). Note that this holds for any combination of decentralized controllers operating in their unsaturated regions. Thus, if the PI controllers can be tuned so that all solutions to (17) are stable, overvoltages will be mitigated. This statement holds even in the presence of controller saturation, which the following reasoning shows.

3.1. Impact of saturation

The proposed control method is affected by two types of saturation, hereafter referred to as *short-term* saturation and *long-term* saturation. Short-time saturation is a temporary result of (1) rate-of-change limitations, or (2) PI controller overshoot, i.e. when $\delta p^{gen}_k = -\tilde{p}^{gen}_k (\delta p^{gen}_k = 0)$ while $v_k < v^{max}_{grid,k} (v_k > v^{max}_{grid,k})$. However, given proper use of an anti-windup scheme, this is of lesser concern from a long-term stability perspective.

Potentially more challenging is the long term saturation which occurs when $\delta p^{gen}_k = -\tilde{p}^{gen}_k (\delta p^{gen}_k = 0)$ while instead $v_k > v^{max}_{grid,k} (v_k < v^{max}_{grid,k})$ for $t_j : j \rightarrow \infty_+$. This represents the inability to either mitigate overvoltage or undervoltage (here meaning any voltage lower than the upper limit). Only the first case is relevant as increasing voltages is not a control objective in this paper. It is however of interest to ensure that uncontrolled voltages always remain above the lower network limit.

By making three assumptions about the radial DN model we can argue that long-term saturation such that $\delta p^{gen}_k = -\tilde{p}^{gen}_k$ for $t_j : j \rightarrow \infty_+$ is nonexistent in the presented control scheme. We can then show that no actions by the decentralized controllers lead to violations of the lower voltage constraint.

Assumption 1. active and/or reactive power injections at one bus increase the voltage at all buses, except the slack bus.

Assumption 2. the reactive power injections to the network are small compared to the active power injections.

Assumption 3. the bus voltages are within the network limits when there are no active or reactive power injections from DERs.

The first assumption is feasible if all voltage sensitivity elements $\frac{\partial v_h}{\partial p_k}, \frac{\partial v_h}{\partial q_k}$ are positive and $\tilde{K}^c$ is a positive matrix. Combined with the second assumption, it is inferred that if the maximum network voltage is above the slack bus voltage, it cannot be higher the maximum generation bus voltage. Conversely, the minimum network voltage, if below the slack bus voltage, cannot be lower than the lowest load bus voltage. Finally, we assume that the grid in question meets the voltage requirements for operation without DERs, which is true for a majority of existing DNs.

Now consider a network of l load buses and $m+n$ buses with controllable DERs so that system operation is stable for any combination of controllers in unsaturated operation.

- If the controllers at m nodes where $v_i > v^{max}_{grid,i}$ at an instance t_s operate linearly, then before some $t_f > t_s$ the voltage at the buses become $v_i \leq v^{max}_{grid,i}$, $i = 1, \dots, m$.
- If the controllers at n buses where $v_j > v^{max}_{grid,j}$ are all in a saturated state at t_s such that $\delta p^{gen}_j = -\tilde{p}^{gen}_j$, then the bus voltages are guaranteed to reach $v_j \leq v^{max}_{grid,j}, j = m+1, \dots, n$ since if full curtailment remains at t_f, the maximum network voltage cannot be higher then what is found at (at least) one generation bus $v_i = v^{max}_{grid,i}$.
- The noncontrollable voltages at l buses are altered by the actions at the $m+n$ buses such that $v^{max.\,load}_{no\,gen.,k} \leq v_k \leq v^{max.\,gen}_{no\,load,k}$, $k = m+n+1, \dots, l$. If $v^{max.\,load}_{no\,gen.,k} < v^{slack}$ is the lowest possible network voltage and Assumption 3 holds, no action taken by $m+n$ controllers will result in a lower voltage constraint violation.

3.2. Closed loop stability

The system matrix for any system (17) has the form

$$\begin{bmatrix} \alpha\hat{K}^c & \hat{K}^c & \beta\hat{K}^c \\ \alpha I & I & \beta I \\ I & 0 & 0 \end{bmatrix}, \tag{22}$$

where I is the identity matrix and 0 a square zero matrix. (22) has k eigenvalues λ_i and (17) is asymptotically stable $iff |\lambda_i| < 1$, $i = 1, \dots, k$[23]. Thus, stability depends only on K^c and the selection of the control parameters α and β. The system matrices (22) for every piecewise linear system (17) describe all possible interactions of unsaturated PI controllers (11) resulting from decentralized control of the system (13). Therefore, control performance can be evaluated with standard linear methods and PI controller design can be based on a selected operational scenario. The feasibility of the design can subsequently be verified by evaluating local system stability for all possible operating conditions through eigenvalue analysis as described above. In practice, this approach might be overly conservative as the physical structure of a network ultimately determines the existence of a specific combination of controllers in parallel unsaturated operation. Network and equipment characteristics also bound the overall performance of the control scheme. Hence, it cannot be guaranteed that specific controller performance criteria always can be met. However, using the proposed modelling framework, stability of the control method in an arbitrary radial DN can easily be evaluated by variation of the voltage sensitivities in K^c, and during changing operating conditions, by varying the sizes of $\hat{K}^c$ and (22).

4. Case study

In this section we demonstrate the functionality of the proposed method and investigate controller interaction in a medium voltage test system.

4.1. Test network

The Cigre European MV benchmark system [19] consists of two radial feeders. The feeder shown in Fig. 1 represents a rural network of two 20 kV load buses connected to a 110 kV network. We add two controllable wind power plants to buses 1 and 2 and study one case where the installed capacity is 4+4 MW *(Case 1)* and one where it is set to 6+1 MW *(Case 2)*. In both cases, during moderate to high generation periods the loads at buses 1 and 2 are negligible from a voltage perspective. The upper voltage is limit set to 1.05 pu.

As the test network is a balanced and symmetric radial DN, we create a model of the complete system according to Section 2 — more specifically (17). The general results from Section 3.2 can then be applied to conduct a stability analysis. The test system is also separately modelled in DIgSILENT PowerFactory, with the controller model (11), (12) stored in an external Python package. Subsequent evaluations of controller dynamic performance are made through nonlinear load flow simulations in PowerFactory, where the controllers are called in an iterated loop. Thus, synchronized updates of DER set points are achieved under the assumptions presented in Section 2.1.

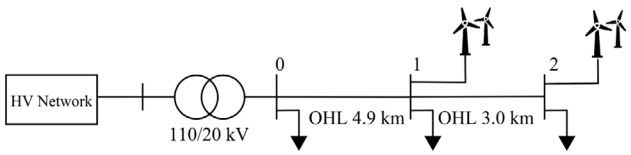

Fig. 1. Modified Cigre MV benchmark feeder diagram. The load at bus 0 represents the aggregated load for all parallel MV feeders.

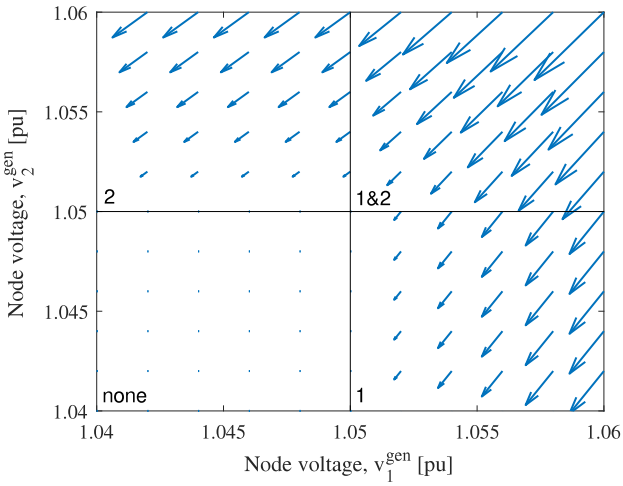

Fig. 2. Case 1: initial control response to theoretical voltage steps, starting from an acceptable voltage level. Arrows indicate change from step voltage to voltage level after first controller curtailment action. The four response regions show buses where a local controller is initially activated.

4.2. Stability and performance considerations

The voltage sensitivity matrix used for the theoretical evaluation is obtained from numerical simulation of Case 1 for an operating point in PowerFactory. The design parameters are set to $\alpha = -1.2\beta$, $\beta = 2$. Initially the reactive power support is deactivated, i.e. $C^{pf} = 0$. It is then verified that the eigenvalues of (22) are in the stability region for all combinations of unsaturated PI controller operation.

The initial control response to a sudden voltage increase is shown in Fig. 2. Here, the system initially has acceptable voltages and the PI controllers are limited to $\delta p_i^{gen} = 0$. Step changes to 100 combinations of node voltages are then achieved through steps in the DER active power injection. Note that some of the resulting voltage combinations are unlikely or even not feasible due to physical network limitations. Four initial response regions are shown in Fig. 2 as *none, 1, 2,* and *1&2*. When the increased voltage is below 1.05 pu, there is no control response (*none*). In two regions (*1, 2*), one PI controller responds, while in one region both respond (*1&2*). Any active control response reduces the voltage at both nodes, as is expected as per Assumption 1. The response direction naturally depends on the voltage sensitivity matrix.

The modelled PI controller behaviour near equilibrium, given constant potential active power injections, is visualized through the linearly interpolated trajectories in Fig. 3, where $1.055 < v_i(0) \leq 1.070$ pu. Unsaturated operation of at least one controller occurs in three response regions, corresponding to three linear systems (18). Three types of locally stable equilibrium points, or attractors, are present. Each attractor has a *basin of attraction*, a zone where all $v_i(0) \to v_i^*$ as $t \to \infty_+$. Two attractors consist of a set of points along straight lines such that $(v_i^{gen,*}, v_j^{gen,*}) = (v_{grid,i}^{max}, < v_{grid,j}^{max})$. The third attractor is a single equilibrium point in $(v_i^{gen,*}, v_j^{gen,*}) = (v_{grid,i}^{max}, v_{grid,j}^{max})$ and is the only equilibrium where both controllers remain in unsaturated operation. Fig. 3 shows that in case of an initial response involving a single unsaturated controller, a single linear model (17) describes

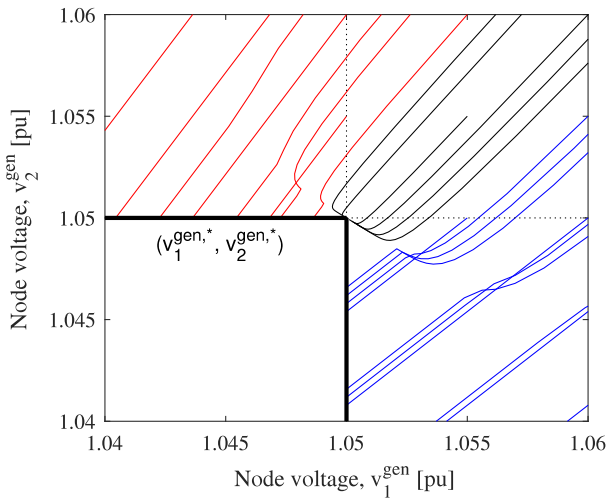

Fig. 3. Case 1: voltage trajectories from control response to theoretical voltage steps. Bold lines indicate location of attractors. Coloured lines indicate the different basins of attraction. Dashed lines indicate the initial response regions.

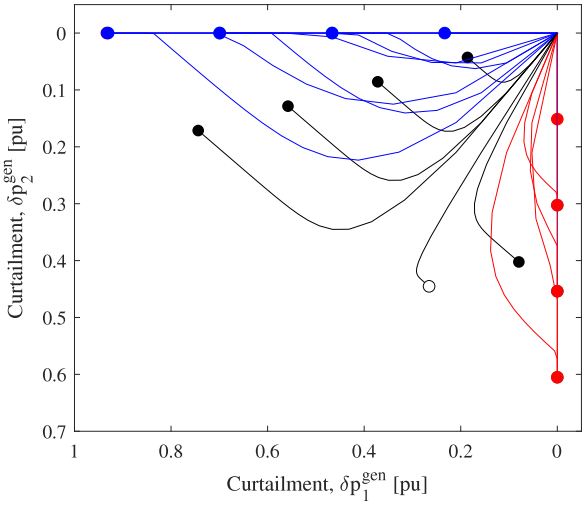

Fig. 4. Case 1: curtailment trajectories. Dots indicate equilibrium points. Coloured lines indicate the different basins of attraction of the voltage attractors. The white dot corresponds to the equilibrium in the example discussed in Section 4.3.

the dynamics along the entire trajectory. In case of an initial double PI controller response, the voltage difference between the two controlled buses in the starting point determines the equilibrium of each trajectory. Only if the difference is small, a single linear model describes the dynamics along the entire trajectory and there exists an equilibrium where both PI controllers remain unsaturated. Otherwise, one of the controllers will reach saturation and a second linear model is needed to describe the system close to the equilibrium. The curtailment trajectories corresponding to the voltage trajectories in Fig. 3 are shown in Fig. 4. The voltage difference between the two buses at the starting point clearly also influences the location of the curtailment equilibrium.

We then investigate the dynamic performance of the PI controllers derived from the linearized model. A nonlinear iterated power flow simulation of Case 2 is conducted using an arbitrary generation profile spanning over a range of operating conditions, including a sudden spike in the DER output. The daily load profile is obtained from [19]. The robustness of the control method is demonstrated by reusing the controller settings from Case 1. In Fig. 5, the active power injection at bus 1 increases at t_a, which raises the feeder positive sequence rms voltage level during a $\sim$ 60 minute period. The PI controllers react

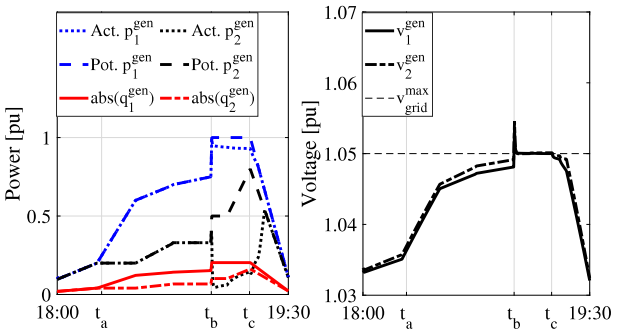

Fig. 5. Case 2: simulated dynamic performance of local voltage controllers in modified Cigre MV test system. DER power injections (left) and corresponding positive sequence rms bus voltages (right).

Table 1
Case 1: theoretical impact of reactive power on voltage and curtailment at bus 1 (bus 2) of the modified Cigre mv test system.

Power Factor	$\|Q\|$ [pu]	Uncontrolled Voltage [pu]	Curtailment Equilibrium [pu]
1.00	0.00 (0.00)	1.065 (1.070)	0.26 (0.44)
0.98	0.20 (0.20)	1.050 (1.053)	0.00 (0.09)
0.95	0.33 (0.33)	1.041 (1.042)	0.00 (0.00)

only when overvoltage is detected (at t_b) and the voltage is rapidly suppressed. The voltage is then limited during a $\sim$ 15 minute period ($t_b \rightarrow t_c$), even with an increase of the potential active power injection at bus 2. The delta control strategy enables accurate estimation of the curtailed energy, as it is equal to the area bounded by potential and actual active power output curves.

4.3. Reactive power support

In Fig. 5, reactive power support is activated by letting $C^{pf} = -0.203$, corresponding to a 0.98 power factor with respect to the maximum potential DER active power output. The R/X ratio of the overhead lines in the test system in Fig. 1 is 1.4. Thus, a nonunity power factor set point is here a relatively effective tool for suppressing the voltage magnitudes, which reduces the need for curtailment. This is exemplified in Table 1 using the trajectory for a modelled equilibrium point in Case 1 (see Fig. 4) for reference. In reality, network and converter limitations restrict the range of feasible reactive power injections, as was noted in Section 1.2. This issue is demonstrated through a simulation of Case 2 in which the system corresponding to Fig. 5 is held at the initial loading conditions while DER outputs increase further up to 100%. The power factor set point is then varied. The results, shown in Table 2, illustrate a case where mitigating overvoltage while avoiding overloading of the overhead line [24] between buses 0 and 1 is a nontrivial task. In such cases, desirable network operation could always be achieved by simply removing the reactive power part of the controller and rely only curtailment of active power only, as per Assumption 3 in Section 3.1. However, the positive effects of reactive power support on network voltage levels in both study cases, resulting in reduced curtailment need, as exemplified in Table 1, clearly motivate the adjustment of power factor set points. To simultaneously maintain a sufficient margin to network loading limits then becomes a key challenge.

5. Discussion

The results presented in this paper illustrate the potential to provide local voltage control with stability and performance guarantees. The proposed quasi-dynamic DN model allows for load and generation profiles to be included in iterated load flow simulations, an approach typically suitable for control interactions in a time scale of seconds [25]. Assessing the need to include more detailed modelling of converter dynamics, although out of scope of this work, is a relevant research question. Nevertheless, the nonlinear characteristics of the local controllers is preserved in the model so that comprehensive system stability requirements can be derived analytically.

Table 2
Case 2: simulated impact of reactive power on voltage at bus 1 (bus 2) and line loading of the modified Cigre mv test system.

Power Factor	Uncontrolled Voltage [pu]	Loading OHL 0-1 [%]
1.00	1.071 (1.075)	96.7
0.98	1.058 (1.061)	99.8
0.95	1.050 (1.053)	103.8

While this work mainly focused on interactions of local controllers stemming from adjustments of active power set points, some aspects of the reactive power support scheme that influence the overall controller performance should be mentioned. The reactive power support, as presented in 2.2, can be considered an enhanced power factor voltage control scheme as, through delta control, the power factor set point is made dependent on the potential maximum active power DER output rather than the actual one. In the absence of delta control capabilities, the latter approach can be obtained in (4) by redefining the active power $\tilde{p}_i^{gen}$ such that $\tilde{p}_i^{gen}(t_k) = p_i^{gen}(t_{k-1})$ in the controller model. This action introduces a inverse relation in the utilization of reactive power and curtailment and would therefore likely result in an increased curtailment need compared to the delta control strategy.

Also worth noting is that, since the proposed method allows for the decoupling of P and Q control, other reactive power support strategies, such as volt/var curves, could be implemented in parallel operation with the local PI controller, replacing the power factor set point adjustment. An additional stability analysis, see e.g. [14], should be performed in such cases.

The possibility to implement various reactive power strategies (including the use of a unity power factor) suggests that the proposed control method could easily be adapted to a wide range of regulatory and technological contexts. Given the typical difference in R/X ratios between LV and MV networks, this flexibility can be particularly useful for finding effective solutions for different voltage levels. A more extensive investigation on this topic, also with respect to the impact of the network limitations, as exemplified in 4.3, is needed to get a more comprehensive view of the plug-and-play capability of the local control method. Future applications to consider also include load control and mitigation of undervoltage. A techno-economic assessment of the delta control strategy for curtailment is another relevant research topic.

6. Conclusions

In this paper, we proposed a local voltage control method for converter-based DERs in distribution networks using both active and reactive power. A modelling framework was constructed, where the nonlinear controller dynamics is represented by a piece-wise linear system. We showed that no interactions between decentralized PI controllers lead to instability if local stability is achieved in each linear system, and the proposed method then guarantees mitigation of overvoltage.

A case study, using a modified Cigre European MV test system, showed the influence of a feeder voltage profile on the location of voltage and curtailment equilibria of controlled DERs. Finally, satisfactory controller performance was demonstrated in the studied power flow scenarios.

CRediT authorship contribution statement

Martin Lundberg: Investigation, Software, Data curation, Writing – original draft, Writing – review & editing. **Olof Samuelsson:** Conceptualization, Methodology, Supervision, Resources. **Emil Hillberg:** Conceptualization, Methodology, Supervision.

Declaration of competing interest

The authors declare that they have no known competing financial interests or personal relationships that could have appeared to influence the work reported in this paper.

References

[1] P. Okanik, B. Kurth, J. Harlow, An update on the paralleling of OLTC power transformers, in: 1999 IEEE T&D Conference (Cat. No. 99CH36333), Vol. 2, 1999, pp. 871–875.

[2] CENELEC, Voltage characteristics of electricity supplied by public electricity networks, Standard EN 50160:2010, 2010.

[3] E. Hillberg, H. Pihl, S. Hallhagen, O. Samuelsson, M. Lundberg, M. Mirz, et al., Active network management for all – ANM4L a collaborative research project, in: White Paper, 2020, www.anm4l.eu.

[4] Technical connection rules for MV, 2018, VDE-AR-N 4110.

[5] Grid connection of energy systems via inverters, part 2: Inverter requirements, 2020, AS/NZS 4777.2:2020.

[6] IEEE standard for interconnection and interoperability of distributed energy resources with associated electric power systems interfaces, in: IEEE Std 1547-2018, 2018.

[7] R. Tonkoski, L.A.C. Lopes, Voltage regulation in radial distribution feeders with high penetration of photovoltaic, in: 2008 IEEE Energy 2030 Conference, 2008, pp. 1–7.

[8] E. Demirok, D. Sera, R. Teodorescu, P. Rodriguez, U. Borup, Evaluation of the voltage support strategies for the low voltage grid connected PV generators, in: 2010 IEEE ECCE, 2010, pp. 710–717.

[9] T. Stetz, F. Marten, M. Braun, Improved low voltage grid-integration of photovoltaic systems in Germany, IEEE Trans. Sustain. Energy 4 (2) (2013) 534–542.

[10] A. Samadi, Large Scale Solar Power Integration in Distribution Grids: PV Modelling, Voltage Support and Aggregation Studies, (Ph.D. thesis), KTH, School of Electrical Engineering (EES), 2014.

[11] R. Caldon, M. Coppo, R. Turri, Coordinated voltage control in MV and LV distribution networks with inverter-interfaced users, in: 2013 IEEE Grenoble Conference, 2013, pp. 1–5.

[12] S. Bolognani, R. Carli, G. Cavraro, S. Zampieri, On the need for communication for voltage regulation of power distribution grids, IEEE Trans. Control Netw. Syst. 6 (3) (2019) 1111–1123.

[13] M. Starke, P. Bhowmik, S. Campbell, M. Chinthavali, B. Xiao, R.S. Krishna Moorthy, B. Dean, J. Choi, A plug-and-play design suite of converters for the electric grid, in: 2020 IEEE ECCE, 2020, pp. 2314–2321.

[14] A. Eggli, S. Karagiannopoulos, S. Bolognani, G. Hug, Stability analysis and design of local control schemes in active distribution grids, IEEE Trans. Power Syst. 36 (3) (2021) 1900–1909.

[15] A.T. Procopiou, L.F. Ochoa, On the limitations of volt-var control in PV-rich residential lv networks: A UK case study, in: 2019 IEEE Milan PowerTech, 2019, pp. 1–6.

[16] S.D. Panjaitan, R. Kurnianto, B.W. Sanjaya, M.C. Turner, DC source-based standalone microgrid control using I-PD scheme for a MIMO system, in: 2017 ICON-SONICS, 2017, pp. 18–23.

[17] N. Li, G. Qu, M. Dahleh, Real-time decentralized voltage control in distribution networks, in: 2014 52nd Annual Allerton Conference on Communication, Control, and Computing, Allerton, 2014, pp. 582–588.

[18] N. Stringer, A. Bruce, I. MacGill, N. Haghdadi, P. Kilby, J. Mills, T. Veijalainen, M. Armitage, N. Wilmot, Consumer-led transition: Australia's world-leading distributed energy resource integration efforts, IEEE Power Energy Mag. 18 (6) (2020) 20–36.

[19] Benchmark Systems for Network Integration of Renewable and Distributed Energy Resources, Tech. Rep., (CIGRE, TF C6.04.02) 2014, p. 575.

[20] M. Mirzaei, M. Soltani, N.K. Poulsen, H.H. Niemann, Model based active power control of a wind turbine, in: 2014 American Control Conference, 2014, pp. 5037–5042.

[21] A. Sangwongwanich, Y. Yang, F. Blaabjerg, D. Sera, Delta power control strategy for multi-string grid-connected pv inverters, in: 2016 IEEE ECCE, 2016, pp. 1–7.

[22] I. Elorza, C. Calleja, A. Pujana-Arrese, On wind turbine Power Delta control, Energies 12 (12) (2019) 2344.

[23] T. Glad, L. Ljung, Control Theory. Multivariable and Nonlinear Methods, Taylor & Francis, 2000.

[24] Nexans U.S., ACSR Electrical Data, Data Sheet, 2018.

[25] IEEE Guide for conducting distribution impact studies for distributed resource interconnection, in: IEEE Std 1547.7-2013, 2014, pp. 1–137.